Automatic Detection of Chip Pin Defect in Semiconductor Assembly Using Vision Measurement

Shengfang Lu[1,2], Jian Zhang[3], Fei Hao[4], Liangbao Jiao[1,2]

[1]Artificial intelligence Industrial Technology Research Institute, Nanjing Institute of Technology, Hongjing Road No.1, 211167, Nanjing, China, lshf14240@163.com
[2]Jiangsu Engineering Research Center of IntelliSense Technology and System, Nanjing Institute of Technology, Hongjing Road No.1, 211167, Nanjing, China
[3]Shool of Information and Communication Engineering, Nanjing Institute of Technology, Hongjing Road No.1, 211167, Nanjing, China
[4]Shool of Mechanical Engineering, Nanjing Institute of Technology, Hongjing Road No.1, 211167, Nanjing, China

Abstract: With the development of semiconductor assembly technology, the continuous requirement for the improvement of chip quality caused an increasing pressure on the assembly manufacturing process. The defects of chip pin had been mostly verified by manual inspection, which has low efficiency, high cost, and low reliability. In this paper, we propose a vision measurement method to detect the chip pin defects, such as the pin warping and collapse that heavily influence the quality of chip assembly. This task is performed by extracting the corner feature of the chip pins, computing the corresponding point pairs in the binocular sequence images, and reconstructing the target features of the chip. In the corner feature step, the corner detection of the pins using the gradient correlation matrices (GCM), and the feature point extraction of the chip package body surface using the crossing points of the fitting lines are introduced, respectively. After obtaining the corresponding point pairs, the feature points are utilized to reconstruct the three dimensional (3D) coordinate information in the binocular vision measurement system, and the key geometry dimension of the pins is computed, which reflects whether the quality of the chip pins is up to the standard. The proposed method is evaluated on the chip data, and the effectiveness is also verified by the comparison experiments.

Keywords: 3D reconstruction, chip pin, defect detection, feature extraction, computer vision.

1. INTRODUCTION

In the electronic industry, surface mount technology (SMT) plays an important role in the chip package process, and greatly enhances the efficiency and accuracy of the installed components onto the printed circuit boards (PCB) [1]-[2]. Quad flat package (QFP) is one type of surface mount package, and the pins of QFP are led out from four sides of the chip with "L" shape. This type of chip contains various pins, and the pin bending (warping and collapse) is easy to appear in the packaging process. The defect detection of the chip pin in SMT has important significance in the chip industry manufacturing and automatic assembly process.

Previously, the quality of the chip package was monitored manually, which has low efficiency, bad reliability and cannot meet the requirements of high speed assembly production [3]. With the development of optical sensors and computer technology, quality detection of the PCBs using the automatic optical inspection (AOI) method has become a main stream for the electronic devices in SMT [4]-[6]. Especially, the measurement of key geometric dimensions of chip pins, including the width distance of a pin, the distance

between adjacent pins and the height of pins (whether there is abruption, warping, collapsing or not) and other key dimensions, is an urgent issue to be solved in the current chip packaging process [7]-[8]. The application and promotion of computer vision technology in industry provide an idea for the chip packaging and pin quality detection. Bai et al. [9] introduced a vision measurement method to locate and inspect the ball grid array (BGA) components. Gao et al. [10] proposed a line-based-clustering method to detect the defect of BGA component in SMT. Nuanprasert et al. [11] presented an efficient approach to analyze the X-ray images obtained from arbitrary rotating angles of BGA, in which the authors also solved the general pattern of solder balls arrangement using the Delaunay triangulation technique. In [5], an automated Bayesian visual inspection framework for PCB assemblies was introduced to detect the various shaped circuit elements on multiple scales. In [12], a fuzzy architecture method was presented to inspect the quality of the soldered interconnections. The automatic signal-processing algorithm to calculate the error ratio was developed, such as the laser ultrasound and interferometer and pattern recognition [13]-

[15]. From the earlier analysis, the AOI systems have a great importance in monitoring the quality of the chip.

The chip pins are easy to deform in the packaging process, and the research on the efficient detection of the pin defect is relatively small. Han et al. [16] addressed a template matching method to solve the rectangular-pin-chip position and defect detection problem in SMT. Although the precise positioning of the pin had been obtained, the depth information of the pin in the three dimensional (3D) measurement space was not given, which was unable to detect the abruption, warping and collapse defects of the chip pin. Schmidt [17] introduced a 3D X-ray microscopy imaging with nanometer resolution for detecting failure analysis in the advanced semiconductor packaging process. Lee et al. [18] proposed a vision inspection system to detect the absence defect, the direction and character recognition of the chip in the tape and reel package, but the defects of the chip pins had not been mentioned in the vision system. In fact, failure analysis of the chip pin has become increasingly demanding with the requirements of the higher performance and quality of the chip. Vision analysis method has been applied in the online inspection system due to the fast, noncontact and nondestructive characteristics [19]-[20]. Based on the machine vision system, Xu et al. [21] proposed a polar coordinate transform, smoothness selection, and one-dimensional integral image algorithm to locate the circular mark points of transistor and calculate the orientation of the transistor component.
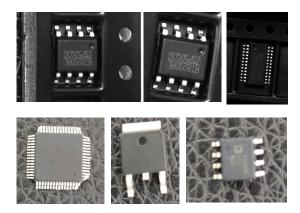

Fig.1. QFP chips with various types.

For the illumination changes, placement angle and complex conditions in the QFP production line, the 3D metric of the chip pin is a difficult task using the vision method. Fig.1. shows the QFP chips with different types and illuminations. In the common solutions of the 3D information [16], [22], it is usually to extract the key point feature, get its pixel coordinates and yield the actual geometric size of the key point using the scaling conversion from pixel to millimeter. The traditional methods have to know the actual physical distance per pixel in advance, which are only suitable for solving the measurement of the feature point in the same plane, but without the depth information. Moreover, the orientation of each chip stored in the slots on the transfer tape is not always facing the same direction [21], which would lead to errors in the corner feature extraction using the customary methods. Especially, the 3D depth information, such as the height and width of the pins, and the distance

between the two adjacent pins, are the most important parameters and indicators in the chip packaging process.

This paper is concerned with the online geometry dimension measurement of the semiconductor chip pins. A binocular vision system, mounted near the transfer tape, is designed to capture the images of the chip and calculate the width and height of the pin, which is used to detect surface defects of the chip pin.

The remaining architecture of this paper is organized as follows. Section II discusses the binocular vision measurement system for measuring the 3D information of the chip pins. Section III presents the corner extraction and the 3D reconstruction algorithm for the corner points on the pins and the surface key points of the chip. Section IV presents the experimental results of the proposed measurement algorithm on the semiconductor chip data. Conclusion and future research work are given in Section V.

2. SYSTEM OVERVIEW

This section aims at introducing a key geometry parameters measurement method of the chip pins based on the binocular vision system in the packaging process. The proposed measurement system, mounted on the conveyor belt, is used to capture images of the chips stored in the tape slots. The vision measurement is suitable for detecting the defect and the geometry in the dynamic conditions [23], [24], which is also applied in many other industrial fields [25]-[27], inspiring us to employ this method. Binocular vision measurement system is briefly discussed in the next subsection. Section II-B discusses the scheme how to extract the corner feature and reconstruct the 3D geometry dimension of the chip in the packaging process.

A. System configuration

Binocular vision measurement system consists of two CCD (Charge Coupled Device) cameras and lighting devices, which are mounted on the transfer tape. Fig.2. shows the vision measurement system configuration of the chip pins geometry dimensions. In the packaging process, the chip is put into the slot on the transfer tape one by one using the nozzle. Before sealing the transfer tape, the vision measurement system is used to capture the chip image and analyze the chip image. When the defect of the chip is detected, the nozzle will pick up the faulty chip and put in a new one. If there are no faulty chips in the field of view (FOV) of the binocular vision cameras, the slots in the transfer tape will be packaged as the conveyor belt moves on.
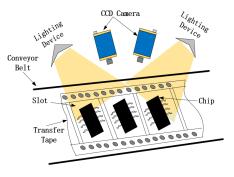

Fig.2. Binocular vision measurement system.

B. *Measurement design*

Vision measurement is commonly used in the precision geometry dimension measurement in both dynamic and static targets [19]-[21]. The principle of vision measurement is by analyzing the images captured via the visual sensors, extracting the key point features and reconstructing the points based on the stereo vision model. In this paper, the chip images in the field of the cameras are first obtained using our proposed stereo vision system. It is easy to determine the chip region of interest (ROI) in the left and right images caught by the left and right cameras. Then, the corner points of the chip pin and the chip plastic surface in the ROI images are extracted and matched, respectively. In this process, we present an algorithm for detecting the key points of the chip. Finally, combined with the binocular camera calibration, we reconstruct the corner points of the pin and the key points on the plastic surface. In the 3D world coordinate system, we use the key points of the plastic surface to form a plane. The defect of the chip pin can be detected by computing the distance from the pin corners to the two dimensional (2D) plane. The 3D reconstruction of chip pin based on binocular vision measurement system is elaborated in Fig.3.
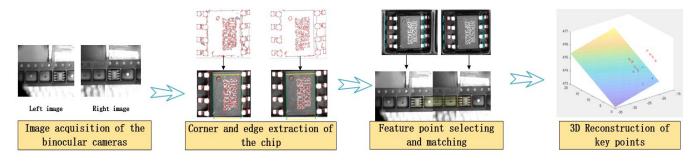

Fig.3. Diagram of chip pin 3D reconstruction based on binocular vision measurement system.

3. FEATURE EXTRACTION & MEASUREMENT

Feature extraction and 3D reconstruction of the key points on the chip are two important factors for detecting the defects of the chip dimension. Hence, in this subsection, we present an effective feature extraction method on the chip pin and the chip plastic surface. Meanwhile, the key dimension measuring algorithm of the chip is also proposed.

A. *Corner extraction of chip pin*

The moving step size of the conveyor belt in practical application is a constant for providing an appropriate perspective of the binocular cameras to capture the images of the chip in the transfer tape slot. Specifically, the position and direction of the chips in the field of view (FOV) are more or less fixed as passing through the vision system when the precise mechanical transmission device moves one step, except for the small inclination of the chip in the slot [13], [18]. In each image of the vision system, the slot region of interest (ROI) of the chip can be obtained according to prior information and experience. The following image analysis is based on the slot ROI, which can save time and improve the processing efficiency.

In defect detection of the chip pins, corner extraction of the pins is a crucial task since the measurement accuracy depends on the pixel position of the target point. Due to the influence of the tape and external light, the contour at both ends of the chip pin sometimes appears elliptical, which results in the false feature extraction of the pin ends. Chip pin target points cannot be accurately and completely extracted using the traditional corner extraction methods [22]-[24], which would greatly affect the reconstruction accuracy of target points. In fact, the characteristics of the chip in the transfer tape include a sharp distinction between pins and background, clear and continuous edges of the pin and plastic surface. Therefore, we first extract the edge contours of pins, and then adopt the corner detection method based on gradient correlation matrices (GCM) [25] of planar curves to locate the corner position.

First, we use the Canny edge detector [26] to extract the contours of the ROI of the chip in the slot. Considering the edge as a regular curve

$$C(t) = (x(t), y(t)) \qquad (1)$$

where t is the parameter of the curve, $x(t), y(t)$ are the coordinate functions, and the gradient vector at any point on the curve is

$$C'(t) = \left(x'(t), y'(t)\right) = (dx, dy) \qquad (2)$$

where dx, dy are the gradients in the x and y directions, respectively.

For a set of points on the curve, with the gradient $(dx_i, dy_i), i = 1, 2, \ldots, k$, the line fits the unit normal vector $\boldsymbol{n}$, the perpendicular distance $d_i(\boldsymbol{n})$ between each point $(dx_i, dy_i,)$ and the fitting line is defined as

$$d_i^2(\boldsymbol{n}) = (\boldsymbol{n}^T[dx_i, dy_i])^2 \qquad (3)$$

To detect the best fitting line, we minimize the following sum of $d_i(\boldsymbol{n})$,

$$\varepsilon^2 = \min(\sum_{i=1}^{k} d_i^2(\boldsymbol{n})) = \min(\boldsymbol{n}^T M \boldsymbol{n}) \qquad (4)$$

where

$$M = \sum_{i=1}^{k}(dx_i, dy_i)^T(dx_i, dy_i) =$$

$$\begin{bmatrix} \sum_{i=1}^{k} dx_i dx_i & \sum_{i=1}^{k} dx_i dy_i \\ \sum_{i=1}^{k} dx_i dy_i & \sum_{i=1}^{k} dy_i dy_i \end{bmatrix} \quad (5)$$

and M denotes the GCM, its eigenvector with the smallest eigenvalue equals to the unit vector normal to the best fit line of the curve.

According to (3) and (5), the minimum eigenvalue of the GCM reflects the feature distribution and the degree of dispersion of the gradient vectors in the gradient plane. By analyzing the determinant of GCM M, the response degree of the corner points of the contour can be calculated, and those ones whose maximum value is greater than the preset threshold are finally selected as the corner. This corner detection algorithm has the characteristics of moderate computational complexity, quality of anti-noise, fast detection speed and good detection effectiveness, which is suitable for the chip pin corner extraction.

According to the above method, we detect all of the GCM corners of the chip in ROI. However, there may be a lot of irrelevant feature points in the ROI, which can be seen in Fig.4.a). In order to select the correct corners of the chip pin, we adopt the prior location information of the chip in the image as the geometry constraint. Due to the precise moving step of the transfer tape, we define the corner of the chip pin in the transfer slots as the corrected target point, which meets the following equation,

$$\begin{cases} a^{(l)} < x_{m,n}^{(l)} < b^{(l)} \\ a^{(r)} < x_{m,n}^{(r)} < b^{(r)} \end{cases} \quad (6)$$

where $x_{m,n}^{(l)}$ is the column pixel coordinate of the GCM corner near the mth row and the nth column in the left part of the chip, $x_{m,n}^{(r)}$ is the pixel coordinate near the ith row and the jth column in the right part of the chip. $a^{(l)}, b^{(l)}$ and $a^{(r)}, b^{(r)}$ are the location constraint thresholds in the left and right regions. Results of the chip pin corners $C_i, (i = 1,2,...,16)$ in Fig.4.a) using the above method are displayed in Fig.4.b).
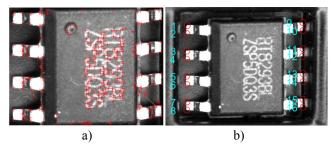

Fig.4. Corner detection of chip pin. a) GCM corners detection; b) Target corners.

B. Feature extraction

The chip plastic surface is seen as the benchmark plane, which is used to calculate the distance from the chip pin corners and determine whether there are non-coplanar faults of the pins. The distances between each pin corner and the chip plastic surface reflect the coplanarity of pin corners,

which can be utilized to detect whether there are faults (such as collapsed foot, broken foot) in the chip. Therefore, feature extraction in the plastic surface is a key step in order to solve the plane equation in the unified 3D world coordinate system. There are four corners intersected by each two lines among the four edges on the plastic surface, which have significant visual edge feature characters. Hence, we first detect the four edge lines on the plastic surface, and then determine the intersection points using the intersecting lines.

As can be seen in Fig.5., the four corners $\#p_1$, $\#p_2$, $\#p_3$, and $\#p_4$ are formed by intersecting the body edges l_1 and l_2, l_2 and l_3, l_3 and l_4, l_4 and l_1, respectively. Due to the saliency of the plastic surface edges, we use the Canny edge and Hough line detection methods to determine the four target edges. The corner $\#p_{w_i}, (w_i = 1,2,3,4)$, is given by

$$\#p_{w_i}: \begin{cases} l_{w_i}: a_{w_i}x + b_{w_i}y + c_{w_i} = 0 \\ l_{w_j}: a_{w_j}x + b_{w_j}y + c_{w_j} = 0 \end{cases} \quad (7)$$

where $(w_i, w_j) = (1,2),(2,3),(3,4),(4,0)$, l_{w_i} and l_{w_j} are the w_ith and w_jth edge equations fitted by using the Canny and Hough methods. a_{w_i}, a_{w_j}, b_{w_i}, b_{w_j} and c_{w_i}, c_{w_j} are the coefficients of the body edge equation.
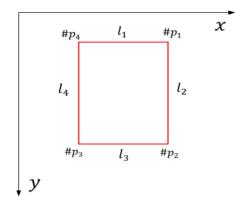

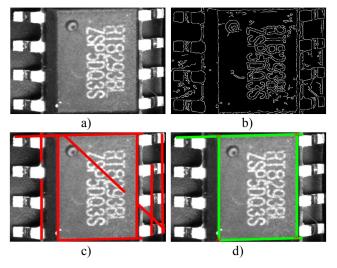Fig.5. Corner extraction of chip plastic surface.

Fig.6. Target edge and corner detection flowchart of chip plastic surface. a) Original image; b) Canny edge detection; c) Edge detection; d) Target edges and corners detection.

Fig.6. indicates the target edge selection process and corner detection result of the chip plastic surface. Canny edges are first detected, and the body edges are selected using the Hough line detection method. The four corners of the surface are finally determined by simultaneously solving the intersecting ones in the four edge equations. In Fig.6.d), the red "∘,+" signs are the four points of intersection between both intersecting edges on the chip plastic surface.

C. 3D measurement

The corners of chip pins and plastic surface are employed to compute the 3D geometry and detect the pin defect. The extracted corners of the chip reflect the profile information, such as the corners $c_1, c_2, ...,$ and c_{16} (as shown in Fig.6.b)) on the chip pins correspond to the principal plane Π defined via the four corners $\#p_1, \#p_2, \#p_3$ and $\#p_4$ (as shown in Fig.7.d)) on the plastic surface. The defect of chip pin is determined by calculating the 3D distance between each pin corner to the plane Π, which is fitted by the four plastic surface feature points. Hence, it is an important work to realize the 3D reconstruction of each feature point and calculate the distances of each pin corner to the plastic surface.

In this paper, we take the chip plastic surface as the reference plane to judge the height (coplanarity) of the chip pins. After obtaining the key feature points, the 3D reconstruction method of the corners using the binocular vision measurement system is performed. Due to the rigidity characteristic of the geometry structure of the chip, the corresponding feature points match in the two images captured via the binocular vision system can be easily achieved. We take the 3D reconstruction of one group of corresponding corner pairs $\#p_i = [u_u^i, v_u^i, 1]^T$ and $\#\bar{p}_i = [\bar{u}_u^i, \bar{v}_u^i, 1]^T$ of the plastic surface edge of the two images as an example. Supposing that the projection matrices from the space point P_i to the two image planes in the binocular vision system are M_1 and M_2, respectively, the following formulas are obtained according to the theory of perspective projection,

$$\lambda_u \begin{bmatrix} u_u^i \\ v_u^i \\ 1 \end{bmatrix} = M_1 \begin{bmatrix} X_u^i \\ Y_u^i \\ Z_u^i \\ 1 \end{bmatrix} = \begin{bmatrix} m_{11}^1 & m_{12}^1 & m_{13}^1 & m_{14}^1 \\ m_{21}^1 & m_{22}^1 & m_{23}^1 & m_{24}^1 \\ m_{31}^1 & m_{32}^1 & m_{33}^1 & m_{34}^1 \end{bmatrix} \begin{bmatrix} X_u^i \\ Y_u^i \\ Z_u^i \\ 1 \end{bmatrix} \quad (8)$$

$$\bar{\lambda}_u \begin{bmatrix} \bar{u}_u^i \\ \bar{v}_u^i \\ 1 \end{bmatrix} = M_2 \begin{bmatrix} X_u^i \\ Y_u^i \\ Z_u^i \\ 1 \end{bmatrix} = \begin{bmatrix} m_{11}^2 & m_{12}^2 & m_{13}^2 & m_{14}^2 \\ m_{21}^2 & m_{22}^2 & m_{23}^2 & m_{24}^2 \\ m_{31}^2 & m_{32}^2 & m_{33}^2 & m_{34}^2 \end{bmatrix} \begin{bmatrix} X_u^i \\ Y_u^i \\ Z_u^i \\ 1 \end{bmatrix} \quad (9)$$

where $[X_u^i, Y_u^i, Z_u^i, 1]$ is the homogeneous coordinate of the space point P_i in the three-dimensional world coordinate system, λ_u and λ_u' are the projection coefficients of the spatial points on the corresponding image planes, M_1 and M_2 are determined by the intrinsic and extrinsic parameters of the corresponding cameras, which can be obtained by using Zhang's camera calibration method [27].

3D reconstruction of each corner can be calculated using the above algorithm. The distance of each chip pin to the plastic surface can also be achieved for detecting the defect of the chip pins. The equation of the chip principle space

plane Π in the 3D coordinate system is fitted using the coordinates of the four spatial points ($\#P_1, \#P_2, \#P_3$, and $\#P_4$) firstly, based on the least squares method. Assume the space principal plane Π equation is obtained by

$$A_\Pi X + B_\Pi Y + C_\Pi Z + 1 = 0 \quad (10)$$

The distance D_d of each spatial pin P_i ($i = 1,2, ...,16$) to the space plane Π in the 3D coordinate system is obtained by

$$D_d = \frac{|A_\Pi X_i + B_\Pi Y_i + C_\Pi Z_i + 1|}{\sqrt{A_\Pi^2 + B_\Pi^2 + C_\Pi^2}} \quad (11)$$

where $P_i = [X_i, Y_i, Z_i], i = 1,2, ...,16,$ is the 3D reconstruction coordinate of the ith chip pin, A_Π, B_Π, C_Π are the equation coefficients of the plane Π in the 3D coordinate system.

The non-coplanar faults of the chip pins occur when the chip pin cocks or bends in the transfer tape slot. It can be detected by monitoring the distance between the pin points P_i and the space principal plane Π and comparing it with the average height.

4. EXPERIMENTS AND EVALUATIONS

A. Experiment configuration

We have tested the proposed method on the chip image data sets, which are placed in the transfer slot. The simulation experiment focused mainly on the robustness of feature extraction, accuracy and precision of the measurement system, and 3D reconstruction performance. Vision sensors of the binocular system are the Basler acA250 CMOS cameras with a maximum frame rate of 20 frames per second. In order to acquire the distinct image of the chip pin and the plastic surface, the RICOH FL-CC2518-5MX lens of high-resolution 25 mm focal length is used in the machine vision systems, which can meet the vision sensors to take the high contrast, sharp images of the chip corners at the working distance. The horizontal and vertical resolutions of the chip image captured by the vision sensor are 2592 x 2048 pixels, which are stored in bmp format. The types of the chip we used in this experiment are QFP RT8293BL and MBI15214GP chips. The ROI selected in the raw image is decided by the location of the chip in the transfer slot.

The simulation and algorithm verification of the proposed measurement system was realized by the MATLAB and OpenCV language programming and executed on the computer workstation with a 3.00 GHz Intel Xeon Gold 6136 processor and 32 GB memory.

B. Comparison of different feature extractions

Due to the strong reflecting of metal root and foot of the chip pin, the stable feature extraction is a difficult and important work for reconstructing the 3D feature points. To verify the robustness of the corner detection of chip pins, we compare our proposed chip pin corner detection method with the state-of-the-art feature extraction method, including the SIFT (scale-invariant feature transform) [24], SURF (speeded up robust features) [23], FAST (features from accelerated segment test) [28], ORB (oriented FAST and rotated BRIEF

[29]) [30], and Harris [22] corner detection. The performance of these methods was evaluated on the same input group of MBI15214GP chip images captured by the left camera.

In Fig.7. the feature points extracted using the SIFT, SURF, FAST and ORB methods are marked with colored circles. The feature detection results of the Harris and our proposed method are marked with red sign "+". As can be seen, the scale invariant features (SIFT and SURF) have good performance in the chip plane due to the multi-scale and multi-resolution representation technology, but have a poor effect on the edge and corner detection. FAST and ORB algorithms have better performance on the corner detection of the chip pins. However, FAST detector has obvious feature response along the edge and detects too many corners, which leads to redundant feature points to be extracted and affects the determination of the pin corners. The Harris corner detection method and our proposed algorithm are both good enough to locate the target points of the chip pins, with the aid of the geometry information of the feature points. However, the time consumption of the Harris corner detection is high with other methods. Extraction efficiency of the chip feature is also an important factor and has a significant influence on the 3D reconstruction. The comparison of the time consumption on the feature extraction of the chips using the above methods is shown in Fig.8.

(a) SIFT

(b) SURF

(c) FAST

(d) ORB

(e) Harris

(f) Our Proposed Method

Fig.7. Comparison of the chip feature points detection using different methods.

According to the figures and comparisons with the existing methods, the proposed method outperforms the state-of-the-art methods in terms of the corner extraction and time consumption, which demonstrate the good performance of the proposed feature detection algorithm on the chip.
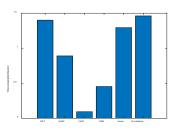

Fig.8. Comparison of the time consumption on the feature extraction of the chip.

C. Accuracy analysis and evaluation of 3D measurement

When the corners of the chip pins and the plastic surface edges are extracted, the matches of the corresponding features between the left and right images captured by the binocular vision system are also determined, due to the rigid structure and prior location information of the chips in the transfer slot. And before this task, the binocular vision system should be calibrated to calculate the intrinsic and extrinsic parameters of the vision sensors using Zhang's method [33]. With the image coordinates of the corners and the calibrated parameters of the cameras, the 3D reconstruction of each feature point is realized using the mathematical model of the binocular stereo vision measurement. According to the size of the chip and the FOV (field of view) of the sensors in our measurement system, the calibration planar target, which is made of special ceramic materials, has a customized size of 8 x 8 grids. The length and width of each square are both 1mm, their machining precision is 0.003 mm. The intrinsic parameters of the left and right cameras are shown in Table 1., the extrinsic parameters of the cameras are shown in Table 2.

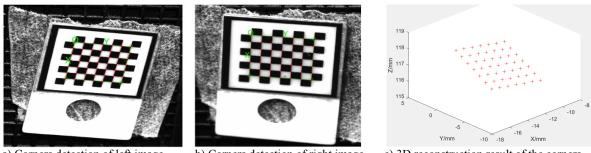Table 1. Intrinsic parameters of the left and right cameras.

Parameter	f_x	f_y	u_0	v_0	k_1	k_2
Left camera	36660	36665	3193.5	864.9	-0.586	16.922
Right camera	25157	24861	3193.5	864.9	0.3115	18.891

Table 2. Extrinsic parameters of the binocular vision system.

$$\boldsymbol{R}_{lr} = \begin{bmatrix} 0.9818 & -0.0027 & -0.1897 \\ 0.0036 & 1.0000 & 0.0045 \\ 0.1897 & -0.0051 & 0.9818 \end{bmatrix}$$

$$\boldsymbol{T}_{lr} = [95.5963, -1.4835, -142.8034]^{\mathrm{T}}$$

where f_x and f_y are the effective focal length in the horizontal and vertical axes in the image coordinate, u_0 and v_0 are the principal point coordinates in the pixel coordinate, k_1 and k_2 are the radial distortion coefficients of the camera. $\boldsymbol{R}_{lr}$ and $\boldsymbol{T}_{lr}$ are the rotation matrix and translation vector between the left and right camera coordinates.
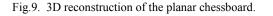
In order to verify the measurement accuracy of our proposed system, the parameters of the standard planar target were regarded as the criterion. The Harris corners of the chessboard were extracted, and the 3D reconstruction of the corners was realized via the binocular vision system. The accuracy of the system was evaluated by comparing the standard and calculated distances of each two corners. The 3D reconstruction result of each corner is shown in Fig.9., the accuracy analysis for the measurement result in the horizontal and vertical directions of the target image is displayed in Fig.10. From the figures, it can be seen that the binocular system has high measurement precision with the maximum error less than $20 \ \mu m$. The results have illustrated that the proposed system has a good performance in 3D reconstruction of the space points.

a) Corners detection of left image,   b) Corners detection of right image.   c) 3D reconstruction result of the corners in the planar target.
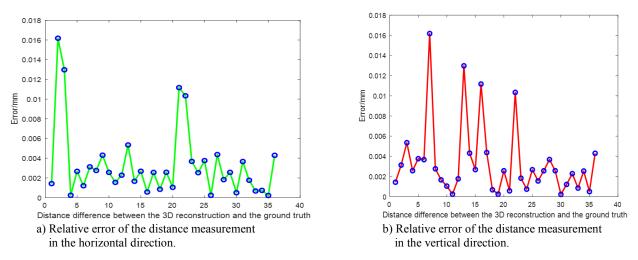
Fig.9. 3D reconstruction of the planar chessboard.

a) Relative error of the distance measurement in the horizontal direction.

b) Relative error of the distance measurement in the vertical direction.

Fig.10. Accuracy analysis of the distance between the 3D reconstruction and the ground truth for each two neighbor corners of the planar chessboard.

D. 3D reconstruction analysis

After verifying the accuracy of the measurement system, we use our proposed algorithm to test the 3D reconstruction effectiveness on the chip images captured by the binocular vision system. In this experiment, we select the 8-pin and 16-pin chips as the test data. The chip images are captured by our measurement system at different time and places of the slot. The corners of the pin and plastic surface in the left and right images are first detected and matched based on the geometry constraints, respectively. Then, all of the target corners are reconstructed in the 3D measurement system, and the ones on the plastic surface are used to fit the principal plane in the 3D coordinate system. The faults of foot warping and fracture can be detected by calculating the distance between the pin corners and the principal plane. In order to verify the 3D reconstruction effectiveness and the robustness of the proposed algorithm, 8 groups of the chip images are selected as the test data set for this experiment. The former 6 groups of the 8-pin chip images are taken by the cameras at different times, and the other 2 groups are the 24 pin chip images. Fig.11. displays the 3D reconstruction result of the key corners and the surface of the chip in the measurement system. Table 2. details the distance of each pin corner to the principal plane. As indicated in the above analysis, the proposed algorithm has high measurement accuracy and stability, which demonstrate that the algorithm has better efficiency and practicability in the 3D measurement and defect detection for a variety of chips.
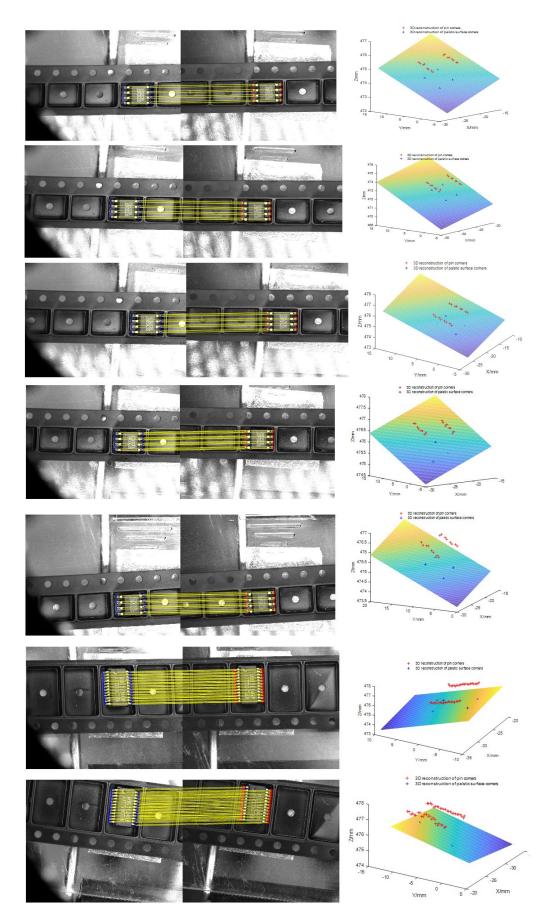
Fig.11. Matching and 3D reconstruction of the key features on a variety of chips.

5. CONCLUSIONS

In this paper, we propose a defect detection system of the chip pins during the semiconductor packing process. The method is developed by the geometric formulation and prior knowledge of the position information of the chips in the transfer slot. Due to the complex light environment, the GCM corner detection of the pin and the feature extraction algorithm of the chip plastic surface are further used to get the key points of the 3D reconstruction process. The proposed system utilizes the 3D coordinate information of the corners and the reconstruction planar of the principal plane to judge the fault of the chip pins. From the validation experiment, the measurement accuracy of the proposed system is up to micro grade. Experimental results have further demonstrated the effectiveness and feasibility of our proposed method on a variety of chips. In the future work, we are going to explore the surface defect detection of the semiconductor chip.

REFERENCES

[1] Zhang, Z.F., Liu, Y., Wu, X.S., Kan, S.L. (2014). Integrated color defect detection method for polysilicon wafers using machine vision. *Advances in Manufacturing*, 2, 318-326. https://doi.org/10.1007/s40436-014-0095-9

[2] Tout, K., Meguenani, A., Urban, J.P., Cudel, C. (2021). Automated vision system for magnetic particle inspection of crankshafts using convolutional neural networks. *The International Journal of Advanced Manufacturing Technology*, 112, 3307-3326. https://doi.org/10.1007/s00170-020-06467-4

[3] Zhou, P., Wang, Z.G., Yan, Y., Huang, N., Kang, R.K., Guo, D.M. (2020). Sensitivity analysis of the surface integrity of monocrystalline silicon to grinding speed with same grain depth-of-cut. *Advances in Manufacturing*, 8, 97-106. https://doi.org/10.1007/s40436-020-00291-5

[4] Song, J.D., Kim, Y.G., Park, T.H. (2019). SMT defect classification by feature extraction region optimization and machine learning. *The International Journal of Advanced Manufacturing Technology*, 101, 1303-1313. https://doi.org/10.1007/s00170-018-3022-6

[5] Acciani, G., Brunetti, G., Fornarelli, G. (2006). Application of neural networks in optical inspection and classification of solder joints in surface mount technology. *IEEE Transactions on Industrial Informatics*, 2 (3), 200-209. https://doi.org/10.1109/TII.2006.877265

[6] Liu, C., Chang, L. (2019). Characterization of surface micro-roughness by off-specular measurements of polarized optical scattering. *Measurement Science Review*, 19 (6), 257-263. https://doi.org/10.2478/msr-2019-0033

[7] Gao, H., Jin, W., Yang, X., Kaynak, O. (2017). A line-based-clustering approach for ball grid array component inspection in surface-mount technology. *IEEE Transactions on Industrial Electronics*, 64 (4), 3030-3038. https://doi.org/10.1109/TIE.2016.2643600

[8] Liu, G., Tong, H., Li, Y., Zhong, H., Tan, Q. (2021). A profile shaping and surface finishing process of micro electrochemical machining for microstructures on microfluidic chip molds. *The International Journal of Advanced Manufacturing Technology*, 115, 1621-1636. https://doi.org/10.1007/s00170-021-07264-3

[9] Acciani, G., Fornarelli, G., Giaquinto, A. (2011). A fuzzy method for global quality index evaluation of solder joints in surface mount technology. *IEEE Transactions on Industrial Informatics*, 7 (1), 115-124. https://doi.org/10.1109/TII.2010.2076292

[10] Liu, S., Ume, I., Achari, A. (2004). Defects pattern recognition for flip-chip solder joint quality inspection with laser ultrasound and Interferometer. *IEEE Transactions on Electronics Packaging Manufacturing*, 27 (1), 59-66. https://doi.org/10.1109/TEPM.2004.830515

[11] Yang, J., Ume, I.C. (2010). Laser ultrasonic technique for evaluating solder bump defects in flip chip packages using modal and signal analysis methods. *IEEE Transactions on Ultrasonics, Ferroelectrics, and Frequency Control*, 57 (4), 920-932. https://doi.org/10.1109/TUFFC.2010.1496

[12] Liu, S., Erdahl, D., Ume, I., Achari, A., Gamalski, J. (2001). A novel approach for flip chip solder joint quality inspection: Laser ultrasound and interferometric system. *IEEE Transactions on Components and Packaging Technologies*, 24 (4), 616-624. https://doi.org/10.1109/6144.974950

[13] Han, B., Yi, M. (2018). A template matching based method for surface-mount rectangular-pin-chip positioning and defect detection. In *2018 Eighth International Conference on Instrumentation & Measurement, Computer, Communication and Control (IMCCC)*. IEEE, 1009-1014. https://doi.org/10.1109/IMCCC.2018.00212

[14] Schmidt, C. (2018). 3-D X-Ray imaging with nanometer resolution for advanced semiconductor packaging FA. *IEEE Transactions on Components, Packaging and Manufacturing Technology*, 8 (5), 745-749. https://doi.org/10.1109/TCPMT.2018.2827058

[15] Lee, J., Han, C., Ko, K., Lee, S. (2016). Development of vision system for defect inspection of electric parts in the tape and reel package. In *2016 16th International Conference on Control, Automation and Systems (ICCAS)*. IEEE, 437-439. https://doi.org/10.1109/ICCAS.2016.7832357

[16] Balter, M., Chen, A., Maguire, T., Yarmush, M. (2017). Adaptive kinematic control of a robotic venipuncture device based on stereo vision, ultrasound, and force guidance. *IEEE Transactions on Industrial Electronics*, 64 (2), 1626-1635. https://doi.org/10.1109/TIE.2016.2557306

[17] Tao, X., Zhang, Z., Zhang, F., Xu, D. (2015). A novel and effective surface flaw inspection instrument for large-aperture optical elements. *IEEE Transactions on Instrumentation and Measurement*, 64 (9), 2530-2540. https://doi.org/10.1109/TIM.2015.2415092

[18] Xu, C., Yang, X., He, Z., Qiu, J., Gao, H. (2021). Precise positioning of circular mark points and transistor components in surface mounting technology applications. *IEEE Transactions on Industrial Informatics*, 17 (4), 2534-2544. https://doi.org/10.1109/TII.2020.2999023

[19] Kurylo, P., Pivarčiová, E., Cyganiuk, J., Frankovský, P. (2019). Machine vision system measuring the trajectory of upper limb motion applying the Matlab software. *Measurement Science Review,* 19 (1), 1-8. https://doi.org/10.2478/msr-2019-0001

[20] Che, J., Sun, Y., Jin, X., Chen, Y. (2021). 3D measurement of discontinuous objects with optimized dual-frequency grating profilometry. *Measurement Science Review,* 21 (6), 197-204. https://doi.org/10.2478/msr-2021-0027

[21] Di Leo, G., Liguori, C., Pietrosanto, A., Sommella, P. (2017). A vision system for the online quality monitoring of industrial manufacturing. *Optics & Lasers in Engineering*, 89,162-168. https://doi.org/10.1016/j.optlaseng.2016.05.007

[22] Harris, C., Stephens, M. (1988). A combined corner and edge detector. In *Proceedings of the 4th ALVEY Vision Conference*. Manchester, UK: Alvety Vision Club, 147-151. http://dx.doi.org/10.5244/c.2.23

[23] Bay, H., Ess, A., Tuytelaars, T., Van Gool, L. (2008). Speeded-up robust features (SURF). *Computer Vision & Image Understanding*, 110 (3), 346-359. https://doi.org/10.1016/j.cviu.2007.09.014

[24] Lowe, D.G. (2004). Distinctive image features from scale-invariant keypoints. *International Journal of Computer Vision*, 60 (2), 91-110. https://doi.org/10.1023/B:VISI.0000029664.99615.94

[25] Zhang, X. Wang, H. Smith, A., Ling, X., Lovell, B.C., Yang, D. (2010). Corner detection based on gradient correlation matrices of planar curves. *Pattern Recognition*, 43 (4), 1207-1223. https://doi.org/10.1016/j.patcog.2009.10.017

[26] Zhao, Y.J., Yan, Y.H., Song, K.C. (2017). Vision-based automatic detection of steel surface defects in the cold rolling process: Considering the influence of industrial liquids and surface textures. *International Journal of Advanced Manufacturing Technology*, 90, 1665-1678. https://doi.org/10.1007/s00170-016-9489-0

[27] Zhang, Z. (2000). A flexible new technique for camera calibration. *IEEE Transactions on Pattern Analysis and Machine Intelligence,* 22 (11), 1330-1334. https://doi.org/10.1109/34.888718

[28] Rosten, E., Porter, R., Drummond, T. (2010). Faster and better: A machine learning approach to corner detection. *IEEE Transactions on Pattern Analysis and Machine Intelligence,* 32 (1), 105-119. https://doi.org/10.1109/TPAMI.2008.275

[29] Calonder, M., Lepetit, V., Strecha, C., Fua, P. (2010). BRIEF: Binary robust independent elementary features. In *Computer Vision – ECCV 2010*. Springer, LNCS 6314, 778-792. https://doi.org/10.1007/978-3-642-15561-1_56

[30] Rublee, E., Rabaud, V., Konolige, K., Bradski, G. (2011). ORB: An efficient alternative to SIFT or SURF. In *2011 International Conference on Computer Vision*. IEEE, 2564-2571. https://doi.org/10.1109/ICCV.2011.6126544